Resveratrol Inhibits Neuronal Apoptosis and Elevated Ca^{2+}/Calmodulin-Dependent Protein Kinase II Activity in Diabetic Mouse Retina

Young-Hee Kim, Yoon-Sook Kim, Sang-Soo Kang, Gyeong-Jae Cho, and Wan-Sung Choi

OBJECTIVE—This study investigated the effects of resveratrol, a natural polyphenol with neuroprotective properties, on retinal neuronal cell death mediated by diabetes-induced activation of Ca^{2+}/calmodulin-dependent protein kinase II (CaMKII).

RESEARCH DESIGN AND METHODS—Diabetes was induced in C57BL/6 mice by five consecutive intraperitoneal injections of 55 mg/kg streptozotocin (STZ). Control mice received buffer. All mice were killed 2 months after the injections, and the extent of neuronal cell death, CaMKII, and phospho-CaMKII protein expression levels and CaMKII kinase activity were examined in the retinas. To assess the role of CaMKII in the death of retinal neurons, a small-interfering RNA (siRNA) or specific inhibitor of CaMKII was injected into the right vitreous humor, and vehicle only was injected into the left vitreous humor, 2 days before death. Resveratrol (20 mg/kg) was administered by oral gavage daily for 4 weeks, beginning 1 month after the fifth injection of either STZ or buffer.

RESULTS—The death of retinal ganglion cells (RGCs), CaMKII, phospho-CaMKII protein levels, and CaMKII activity were all greatly increased in the retinas of diabetic mice compared with controls, 2 months after induction of diabetes. Terminal deoxynucleotidyl transferase (TdT)-mediated dUTP nick-end labeling (TUNEL)-positive signals co-localized with CaMKII- and phospho-CaMKII immunoreactive RGCs. However, in addition to CaMKII knockdown and inhibition by siRNA or a specific inhibitor, respectively, resveratrol provided complete protection from diabetes-induced retinal cell death.

CONCLUSIONS—In the present study, resveratrol prevented diabetes-induced RGC death via CaMKII downregulation, implying that resveratrol may have potential therapeutic applications for prevention of diabetes-induced visual dysfunction. ***Diabetes*** **59:1825–1835, 2010**

Diabetic retinopathy is a major complication of diabetes associated with vascular and neuronal abnormalities, leading to severe visual dysfunction (1–3). Recent studies have emphasized the importance of diabetes-induced neuronal damage in the retina at an early stage of disease progression (2,3–7). The apoptotic cells due to diabetes are likely to include retinal ganglion cells (RGCs) and other neurons (8). Therefore, the identification of pharmacological targets for the prevention of damage to RGCs from diabetes may provide a potential therapeutic strategy for diabetes-induced vision loss.

Ca^{2+}/calmodulin-dependent protein kinase II (CaMKII) is a multifunctional serine-threonine protein kinase that is implicated in a variety of neuronal functions (9–11). Recently, it was found that CaMKII contributes to the death of neuronal cells, including RGCs (10,12–14). However, CaMKII also promotes neuronal survival in response to various stresses (15,16), and thus it has been proposed that CaMKII is an important point of intersection for different pathways involved in neuron-destroying diseases, including diabetic retinopathy.

For prevention of vision loss due to neuronal and vascular damage, topical or oral treatments with ocular penetration are ideal therapies that have been developed recently; in addition, several clinical studies have concentrated on the beneficial effects of natural polyphenols, such as resveratrol (17,18). Resveratrol is a plant-derived phytoalexin with diverse health benefits, including protection from metabolic disorders, such as diabetes (19–21). Although many studies have shown neuroprotective effects of resveratrol in in vitro experimental optic neuropathy (22,23), the effects of resveratrol on retinal neuron damage due to diabetes are not known. Therefore, we investigated whether resveratrol affects CaMKII-dependent RGC death in diabetic mice and found that resveratrol can suppress CaMKII induction and thereby decrease the extent of RGC death. Our results suggest that resveratrol may have powerful therapeutic applications for prevention of CaMKII-mediated RGC death in diabetic retinopathy.

RESEARCH DESIGN AND METHODS

Animals. Male C57BL/6 mice (Samtako, Osan, Korea), weighing 20–22 g (8 weeks old), were used in this study. All mice were maintained on a standard rodent diet (20% protein, 4.5% fat, 6% cellulose, and 7.25% ash [containing 1.2% calcium and 0.62% phosphorus] [#5057; Purina, Kyeonggi-Do, Korea]) and water ad libitum and were handled in strict accordance with the Institutional Animal Care and Use Committee of Gyeongsang National University.

For induction of diabetes, mice were injected intraperitoneally with 55 mg/kg streptozotocin (STZ; Sigma, St. Louis, MO) dissolved in 50 mmol/l sodium citrate (pH 4.5), once a day for 5 consecutive days, and sex- and age-matched control mice received buffer alone. All mice were killed 2 months after the injections. Blood samples were obtained by tail puncture after a 2-h fasting period, and the blood glucose levels were measured using a glucometer (Precision, U.K.). Diabetes was confirmed by blood glucose levels >13.9 mmol/l, 1 week after the fifth injection of STZ. Body weights and blood glucose levels in mice were recorded every 2 weeks.

Administration of resveratrol. Resveratrol (*trans*-3,4′,5-trihydroxystilbene; category R5010; Sigma; 20 mg/kg) was suspended in 0.5% carboxymethylcellulose (CMC; Sigma) dissolved in 0.9% saline. This solution was administered by oral gavage once a day for 4 weeks, beginning 1 month after the fifth injection of STZ or buffer, and 0.5% CMC was given as a control. Finally, mice were assigned to four groups (that is, control and diabetic mice treated with

From the Department of Anatomy and Neurobiology, Gyeongsang National University, Jinju, Gyeongnam, Korea.
Corresponding author: Wan Sung Choi, choiws@gnu.ac.kr.
Received 25 September 2009 and accepted 17 April 2010. Published ahead of print at http://diabetes.diabetesjournals.org on 27 April 2010. DOI: 10.2337/db09-1431.

TABLE 1
Changes in body weight and blood glucose level with resveratrol treatment

	Body weight (g)				Blood glucose (mmol/l)			
	C-C	C-R	D-C	D-R	C-C	C-R	D-C	D-R
Week 0	28.3 ± 0.3	27.7 ± 0.5	21.2 ± 0.5	20.4 ± 0.4	8.7 ± 0.1	9.0 ± 0.3	25.4 ± 0.8	27.5 ± 0.9
Week 2	27.6 ± 0.3	26.3 ± 0.4	21.1 ± 0.6	21.1 ± 0.5	9.0 ± 0.2	7.4 ± 0.2	31.8 ± 0.7	29.6 ± 0.8
Week 4	28.5 ± 0.3	27.8 ± 0.4	20.6 ± 0.6	21.2 ± 0.5	8.3 ± 0.2	7.9 ± 0.2	31.2 ± 0.8	27.7 ± 1.2*

Data are means ± SE ($n = 10$). Resveratrol (in 0.5% CMC) at a dose of 20 mg/kg of body weight and 0.5% CMC alone were administered daily to control and diabetic mice, respectively, by oral gavage for 4 weeks. Time points were 0, 2, and 4 weeks after administration of resveratrol and CMC to control and diabetic mice, respectively, 1 month after STZ treatment: C-C and C-R, CMC- and resveratrol-treated control mice, respectively; D-C and D-R, CMC- and resveratrol-treated diabetic mice, respectively. *$P < 0.05$ compared with CMC- and resveratrol-treated diabetic groups.

either CMC or resveratrol, respectively). After the treatments, changes in body weights and blood glucose levels were recorded every 2 weeks.

Assay kits and antibodies. To detect cell death, we used terminal deoxynucleotidyl transferase (TdT)-mediated dUTP nick-end labeling (TUNEL) assay kits with two different detection modes: Converter-POD and TMR red (In Situ Cell Death Detection kits; Roche, Mannheim, Germany, respectively). CaMKII activity was examined using the CaMKII Kinase Assay Kit from Upstate (Temecula, CA), and an enhanced chemiluminescent (ECL) kit was obtained from Amersham Biosciences (Little Chalfont, U.K.). Mouse and rabbit monoclonal antibodies to CaMKII, phospho-CaMKII (T286), active caspase-3, and gamma synuclein (γ-Syn; the ganglion cell marker) were purchased from Abcam (Cambridge, U.K.). Mouse monoclonal antibodies against α-tubulin and pro-caspase-3 were obtained from Sigma. Secondary horseradish peroxidase (HRP)-conjugated anti-mouse and -rabbit IgGs for Western blotting, a biotinylated anti-rabbit IgG for immunohistochemistry, and Qdot 525 goat F(ab′)$_2$ and Alexa Fluor 594 goat anti-mouse IgGs or Alexa Fluor 350 and 488 goat anti-rabbit IgGs for immunofluorescent staining were purchased from Pierce (Rockford, IL), Molecular Probes (Eugene, OR), Vector Laboratories (Burlingame, CA), and Invitrogen (Carlsbad, CA), respectively.

Western blot analysis. Protein extraction and Western blot analyses were performed as described previously (24). Total protein (30 μg) from the retinas of each group of mice was subjected to 10% SDS-PAGE and then transferred to a nitrocellulose membrane (Millipore). The blots were incubated consecutively in primary antibody against CaMKII, phospho-CaMKII, and pro- or active caspase-3 as well as an HRP-conjugated anti-rabbit IgG, and the target proteins were visualized using an enhanced chemiluminescent kit. Each blot was reprobed with α-tubulin and pro-caspase-3 to control for differences in loading. The fold changes in protein levels compared with controls, normalized to α-tubulin or pro-caspase-3, are indicated below the blots and as a bar graph. Data are representative of four independent tests.

Measurement of changes in retinal morphology. Two months after injection of STZ or buffer, 10-μm frozen retinal sections were prepared as described previously (25). To assess retinal morphological changes, the sections were stained with hematoxylin and eosin (H&E), and retinal thickness was measured as the length (μm) from the ganglion cell layer (GCL) to the tip of the inner nuclear layer. A comparative analysis of the retinal thicknesses in diabetic and control groups was performed using four different fields in four different regions of each retina.

Immunohistochemical staining. Immunohistochemistry was performed in the sectioned retinas as described previously (25). After blocking with serum, the sections were incubated in primary antibody against CaMKII or phospho-CaMKII, a biotinylated secondary anti-rabbit IgG, and an avidin-biotinylated HRP complex (ABC; Vector Laboratories), consecutively. To visualize immunoreactivity to CaMKII, the sections were developed using 0.025% 3,3′-diaminobenzidine tetrahydrochloride (DAB; Sigma)/0.003% H_2O_2 and counterstained with cresyl violet to dye neuronal cells. To confirm whether the immunopositive cells of CaMKII and phospho-CaMKII were RGCs, we performed double-immunofluorescent staining as described previously (24) for CaMKII or phospho-CaMKII and γ-Syn. Retinal sections were incubated consecutively in Image-iT FX signal enhancer (Molecular Probes) for 10 min, a mixture of primary antibodies for 2 h, and a mixture of Alexa Fluor 350 and 594 goat anti-rabbit and mouse IgGs for 1 h. The sections were then counterstained with the nuclear marker 40,6-diamidino-2-phenylindole dihydrochloride (DAPI; Invitrogen) and wet-mounted in ProLong Gold antifade reagent (Invitrogen).

Evaluation of cell death using TUNEL assays. Cell death was analyzed in the retinal cryosections using the TUNEL assay kit with Converter-POD according to the manufacturer's directions. The sections were fixed in 10% fresh formaldehyde for 20 min at room temperature, washed three times in 100 mmol/l PBS (PBS; pH 7.4) for 3 min, incubated in blocking solution (3% H_2O_2 in methanol) for 10 min, permeabilized in 0.1% Triton X-100 with 0.1% sodium citrate in PBS for 5 min on ice, and washed again in PBS. The fixed and permeabilized sections were covered with parafilm and consecutively incubated in the TUNEL reaction mixture for 1 h and Converter-POD for 30 min at 37°C. After washing in PBS, the signal-converted sections were developed using DAB substrate with H_2O_2 in PBS and counterstained with cresyl violet. To confirm whether the TUNEL-positive cells are RGCs or phospho-CaMKII–immunopositive cells, we sequentially performed immunofluorescent staining as described previously (24) for γ-Syn and phospho-CaMKII and the TUNEL assay with TMR red according to the manufacturer's directions on the same cryosections. Retinal sections were incubated consecutively in signal enhancer, primary antibody for γ-Syn, and phospho-CaMKII for 2 h and Alexa Fluor 488 goat anti-rabbit IgG for 1 h. The sections were then stained with the TUNEL reaction and counterstained with DAPI. To determine the correlation between RGC death and CaMKII or phospho-CaMKII expression, double-immunofluorescent staining for CaMKII or phospho-CaMKII and γ-Syn, using Qdot 525 and Alexa Fluor 350 goat anti-mouse and rabbit IgGs and the TUNEL reaction, were sequentially performed as mentioned above. All reactions were performed in a moist chamber to prevent evaporative loss. The total number of TUNEL- and CaMKII or phospho-CaMKII–positive RGCs was counted in the GCL (~100 μm) in four different fields from three different retinas for each group.

Knockdown and inactivation of CaMKII. For knockdown of CaMKII, we performed target gene silencing with a small-interfering RNA (siRNA). The sequence of αCaMKII siRNA for silencing the mouse CaMKII was designed using the Turbo si-Designer program (Bioneer; Daedeok-gu, Daejeon, Korea), and the siRNA duplex was purchased from Bioneer. The sense and antisense sequences of the siRNA were as follows: 5′-UGAUCGAAGCCAUAAG CAA(dTdT)-3′ (sense) and 5′-UUGCUUAUGGCUUCGAUCA(dTdT)-3′ (antisense). The siRNA duplex was completely dissolved in RNase-free distilled water at a final concentration of 1 mmol/l and diluted again to 1/10 and 1/100 (0.1 and 0.01 mmol/l). To select the best condition for siRNA gene silencing, 2 μl each siRNA diluent were carefully injected into the right vitreous humors of mice 2 months after induction of diabetes, and 2 μl distilled water was injected into the left vitreous humors as controls as described previously (7). Mice were killed 0, 1, 2, and 4 days after the injections, and the efficiency of the siRNA was determined by Western blotting of CaMKII. Data are representative of four independent tests.

To examine the effects of CaMKII inhibition, a myristoylated autocamtide-2–related inhibitory peptide (AIP) (Biomol, Plymouth Meeting, PA), a highly specific and potent inhibitor of CaMKII, was completely dissolved in sterile PBS (pH 7.4) at a final concentration of 500 μmol/l. AIP (2 μl) was injected into the right vitreous humors of mice 2 months after induction of diabetes, and PBS was injected into the left vitreous humors as controls. The efficiency of the AIP was determined by Western blotting of CaMKII 0, 1, 2, and 4 days after the injection. Data are representative of four independent tests.

Finally, 1 mmol/l siRNA or 500 μmol/l AIP was injected intravitreally into the retinas of mice 2 months after injection of STZ or buffer, and changes in the expression levels of CaMKII and phospho-CaMKII, the kinase activity of CaMKII, and the extent of cell death by CaMKII knockdown and inhibition were evaluated after 2 days of treatment.

CaMKII kinase assay. CaMKII kinase activity was analyzed in 100 μg total protein from each retina by the CaMKII Kinase Assay Kit (Upstate) according to the manufacturer's directions with autocamtide-3 as a specific substrate for CaMKII. CaMKII was stimulated with buffer containing 40 mmol/l HEPES, 1 mmol/l Mg-acetate, 100 μmol/l EGTA, 200 μmol/l Ca^{2+}, 50 μmol/l ATP, and 10 μmol/l calmodulin. The reaction was initiated by the addition of calmodulin and terminated by the addition of 1 mmol/l EGTA at the indicated times. The results are reported as total enzyme activity in the presence of exogenous Ca^{2+} and calmodulin and expressed in picomoles phosphate incorporated into

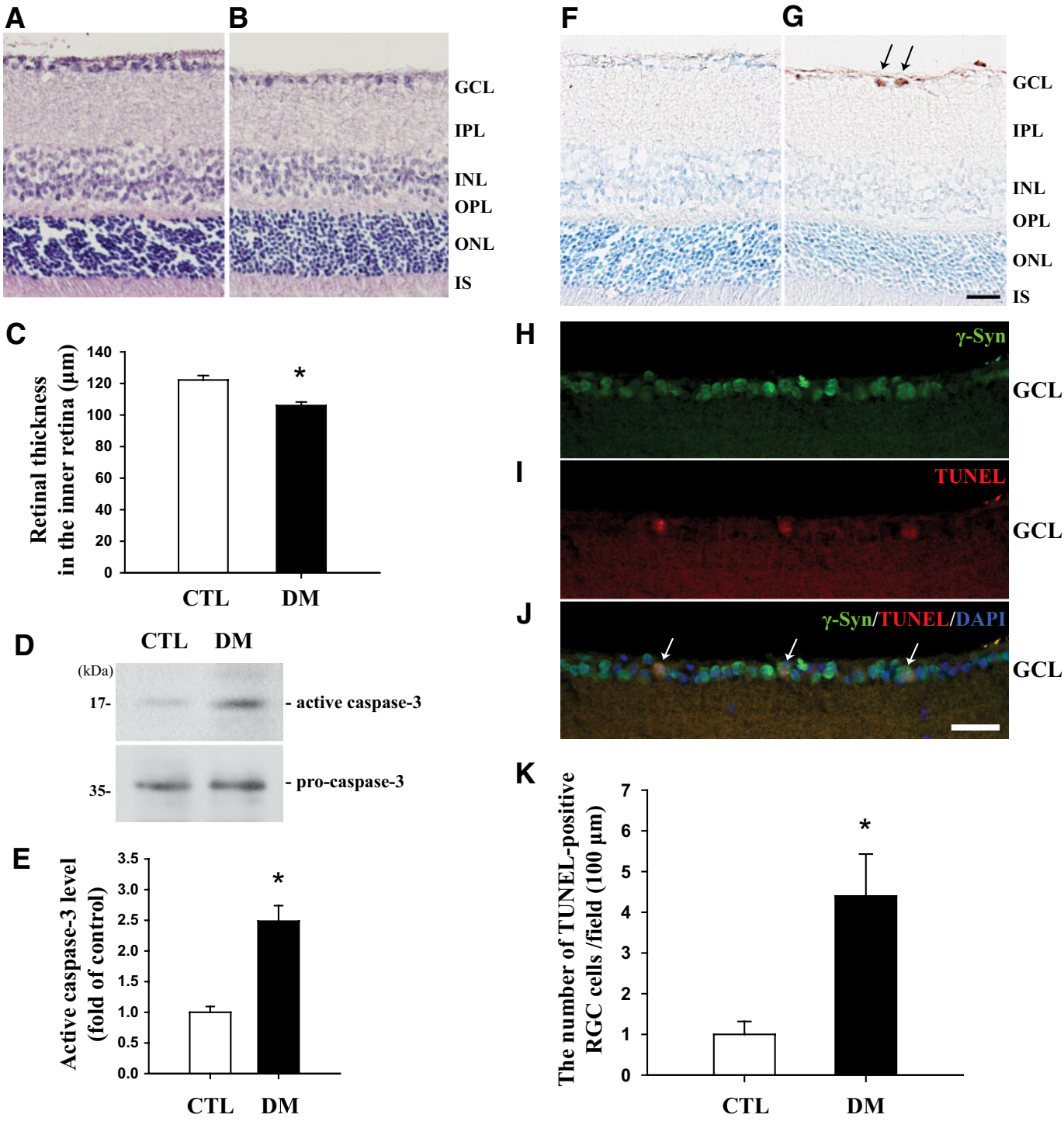

FIG. 1. Determination of retinal thickness and neuronal cell death in retinas of mice 2 months after induction of diabetes compared with control mice. For morphological analysis, H&E staining was performed on 10-μm retinal cryosections of control (*A*) and diabetic (*B*) mice. Retinal thickness was measured as the length (in μm) from the GCL to the tip of the INL, and the results were obtained from comparative analysis of four different images of each retina (*C*). To assess cell death induced by diabetes in the retinas, Western blotting using an antibody to active caspase-3 was performed for the retinas of both groups (*D*). An immunoblot with an antibody to active caspase-3 was reprobed with an antibody to pro-caspase-3 to control for differences in loading, and the level of each protein was normalized to that of pro-caspase-3. Four independent tests were repeated in different retinal extracts from each group, and the results are indicated as the fold change (*E*). To investigate retinal neuron death, the TUNEL assay was performed on retinal sections from control and diabetic mice, followed by counterstaining with cresyl violet (*F* and *G*). To confirm the death of RGCs, immunofluorescent staining of γ-Syn, the GC marker, using Alexa Fluor 488 goat anti-rabbit IgG (*green*) and TUNEL staining were performed consecutively on the same sections from diabetic mice, and the sections were counterstained with the nuclear marker DAPI (*H–J*). The total number of TUNEL$^+$ RGCs was counted in four different fields of the GCL (~100 μm) from three different retinas of each group (*K*). Data are means ± SE ($n = 4$). *$P < 0.05$ comparing control and diabetic groups. CTL and DM, control and diabetic mice 2 months after injection of buffer or STZ; INL, inner nuclear layer; IPL, inner plexiform layer; IS, inner segment; ONL, outer nuclear layer; OPL, outer plexiform layer. Bars, 12.5 μm. (A high-quality digital representation of this figure is available in the online issue.)

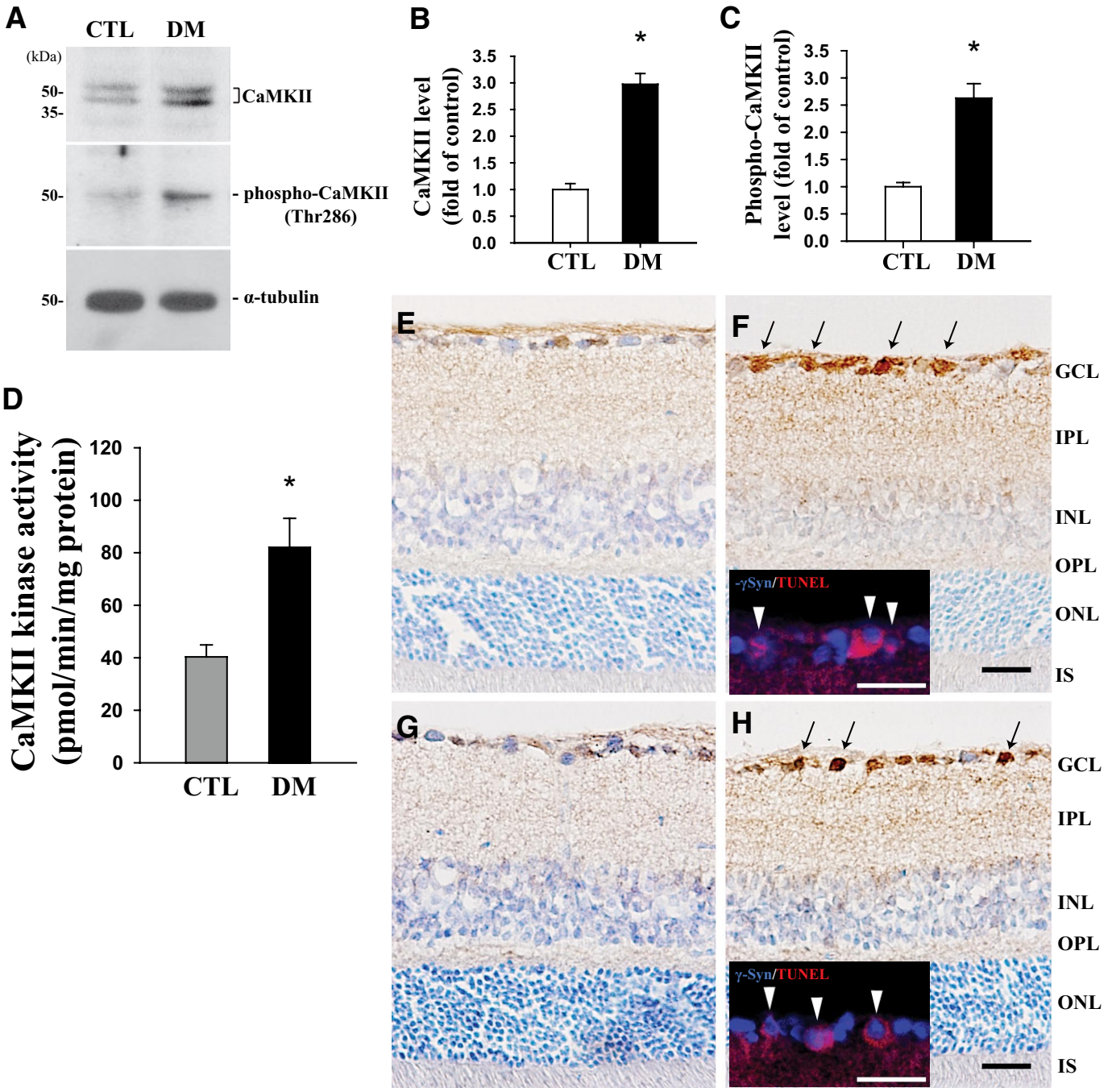

FIG. 2. Molecular and morphological expression of CaMKII and phospho-CaMKII (Thr286), and CaMKII kinase assay in retinas of mice 2 months after induction of diabetes compared with controls. Protein levels of CaMKII and phospho-CaMKII were assessed by Western blotting using 30 μg total protein from each retina, and representative blots from four independent Western blots are shown in *A*. The immunoblots were reprobed with α-tubulin to control for differences in loading, and levels of each protein were normalized to that of α-tubulin. The results indicate the fold change in *B* and *C*, respectively. Analysis of CaMKII kinase activity was performed in the same retinal homogenates (100 μg) prepared for immunoblotting using the CaMKII Kinase Assay Kit. The results are expressed as picomoles of phosphate incorporated into the CaMKII substrate peptide per minute per milligram total protein, and four independent tests were repeated with different retinal extracts for each group (*D*). Data are means ± SE ($n = 4$). *$P < 0.05$ comparing control and diabetic groups. To confirm the distribution of CaMKII (*E* and *F*) and phospho-CaMKII (*G* and *H*) in retinal neuronal cells from control and diabetic mice, retinal cryosections were immunostained with each antibody and then counterstained with cresyl violet. Arrows indicate immunopositive signals of CaMKII and phospho-CaMKII in the GCL of the diabetic retina, and arrowheads in each insert show the double-immunofluorescent staining of γ-Syn and CaMKII or phospho-CaMKII, using Alexa Fluor 350 (*blue*) and 594 (*red*) goat anti-rabbit and mouse IgGs (*F* and *H*). CTL and DM, control and diabetic groups 2 months after injection of buffer or STZ; INL, inner nuclear layer; IPL, inner plexiform layer; ONL, outer nuclear layer; OPL, outer plexiform layer. Bars, 12.5 μm. (A high-quality digital representation of this figure is available in the online issue.)

autocamtide-3 per minute per milligram total retinal protein. Four independent tests were repeated in different retinal extracts for each group.

Image capture and statistical analyses. All retinal images were captured at a distance of ~0.8–1 mm from the optic nerve head using an IX2-DSU disk scanning biological microscope (Olympus, Wendenstrasse, Hamburg, Germany). Quantitative analyses were performed using the Soft Imaging System (System, Münster, Germany) and SigmaGel 1.0 software (Jandel Scientific, Erkrath, Germany), and bar graphs were constructed using SigmaPlot 4.0 (SPSS, Chicago, IL). All data are representative of four independent values and presented as means ± SE. Statistical analyses were performed nonparametri-

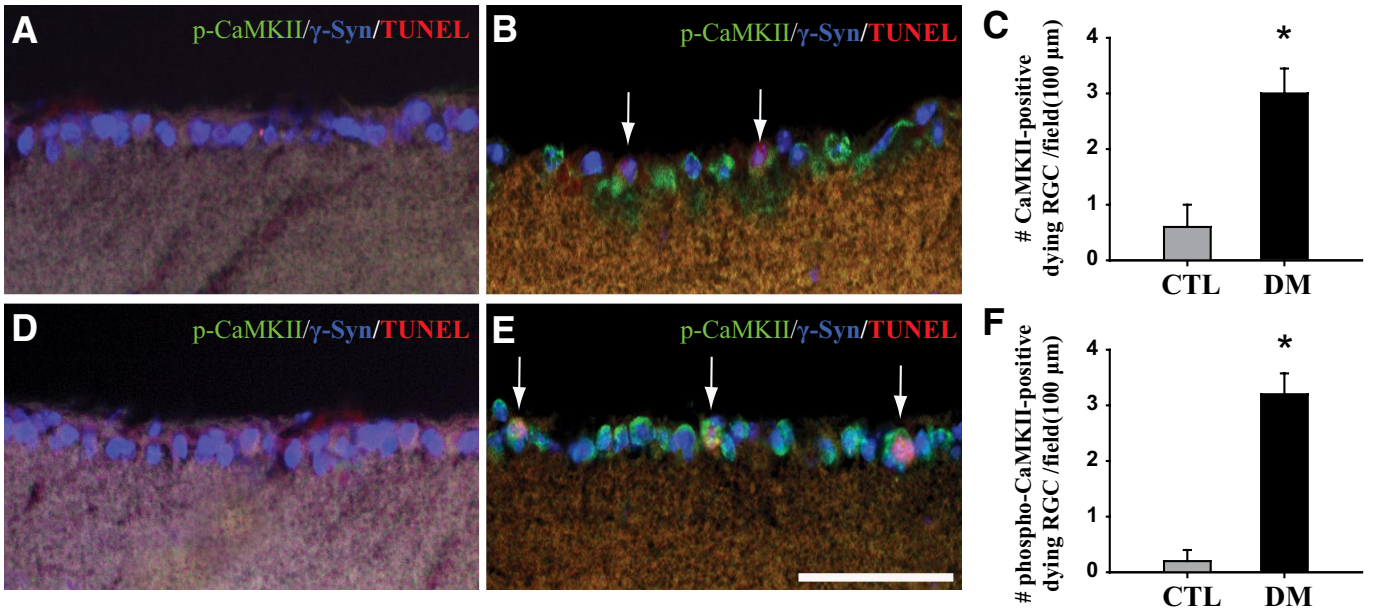

FIG. 3. Co-localization of CaMKII or phospho-CaMKII immunopositive signals and apoptotic RGC cells in retinas of mice 2 months after induction of diabetes compared with controls. To examine the correlation between CaMKII or phospho-CaMKII expression and RGC cell death, double-immunofluorescent staining for CaMKII or phospho-CaMKII and γ-Syn, the ganglion cell marker, using Qdot 525 (*green*) and Alexa Fluor 350 (*blue*) goat anti-mouse and rabbit IgGs, and TUNEL staining (*red*) were sequentially performed on the same sections. Arrows in *B* and *E* indicate TUNEL-positive RGC cells that were immunopositive for CaMKII and phospho-CaMKII in the diabetic retinas compared with control (*A* and *D*). The total number of triple-labeled cells was counted in the GCL (~100 μm) in four different fields from three different retinas for each group (*C* and *F*). Data are means ± SE (n = 4). **P < 0.001 comparing control and diabetic groups. CTL and DM, control and diabetic mice 2 months after injection of buffer or STZ; INL, inner nuclear layer; IPL, inner plexiform layer; ONL, outer nuclear layer; OPL, outer plexiform layer. Bars, 12.5 μm. (A high-quality digital representation of this figure is available in the online issue.)

cally using the Kruskal-Wallis H test and the Mann-Whitney U test (SPSS). A P value of <0.05 was considered statistically significant.

RESULTS

Control mice exhibited a sustained increase in body weight (g) from the beginning to the end of the study period (21.5 ± 0.38 to 29.4 ± 0.55, $P < 0.05$, $n = 10$), but diabetic mice showed no significant change in weight (data not shown). The blood glucose levels (mmol/l) of diabetic mice increased markedly and steadily from 1 week to 2 months after induction of diabetes (23.3 ± 1.53 to 31.2 ± 0.87, $n = 10$, respectively), although control mice remained normoglycemic throughout the study. Administration of resveratrol and CMC did not affect the body weights of diabetic or control mice, or the blood glucose levels of control mice; however, hyperglycemia was significantly decreased in resveratrol-treated diabetic mice compared with CMC-treated diabetic mice after 2 months (31.2 ± 0.84 vs. 27.7 ± 1.16 mmol/l; $P < 0.05$, $n = 10$) (Table 1).

In H&E staining, mice showed a significant decrease ($P < 0.05$, $n = 4$) in the thicknesses of the inner retina, from the GCL to the tip of the inner nuclear layer, by 13.3% 2 months after induction of diabetes compared with those of controls (Fig. 1*C*). No diabetes-induced changes were observed in the thicknesses of the outer retinal regions (data not shown). In Western blot analysis of active caspase-3 to confirm cell death, protein levels were highly increased (2.5-fold; $P < 0.05$, $n = 4$) in the retinas of diabetic mice compared with controls (Fig. 1*D* and *E*). TUNEL-positive signals were observed in the GCLs of the diabetic retinas (arrows in Fig. 1*G*) compared with controls (Fig. 1*F*) and specific to RGCs (arrows in Fig. 1*J*). The number of TUNEL-positive RGCs was greatly increased (4.4-fold; $P < 0.05$, $n = 4$) in the diabetic retinas compared with controls (Fig. 1*K*).

In Western blotting with CaMKII antibody, we observed two bands (~45 and 54 kDa) for CaMKII protein (Fig. 2*A*), indicating its α and β forms, and the molecular level of CaMKII was considered the total amount of both forms. Protein levels of both CaMKII and phospho-CaMKII (~50 kDa) were greatly increased (2.9- and 2.6-fold; $P < 0.05$, $n = 4$, respectively) in the retinas of diabetic mice compared with controls (Fig. 2*A*–*C*). Likewise, CaMKII kinase activity was significantly greater (2.03-fold; $P < 0.05$, $n = 4$) in the retinas of diabetic mice than in controls (Fig. 2*D*). Immunoreactivities of CaMKII and phospho-CaMKII increased in the GCLs of diabetic retinas (arrows in Fig. 2*F* and *H*) compared with controls (Fig. 2*E* and *G*) and were specific to RGC cells (arrowheads in inserts) (Fig. 2*F* and *H*).

Figure 3 shows that not only were all TUNEL-positive cells RGCs but also the apoptotic RGCs were CaMKII or phospho-CaMKII immunopositive in the retinas of diabetic mice (arrows in Fig. 3*B* and *E*), while the RGCs of control mice were not (Fig. 3*A* and *D*). The number of RGCs co-stained for TUNEL and CaMKII or phospho-CaMKII was greater (2.8- or 5.3-fold; $P < 0.05$, $n = 4$, respectively) in diabetic retinas than in controls (Fig. 3*C* and *F*).

Treatment with siRNA efficiently decreased the level of CaMKII protein in a dose- and time-dependent manner and was greatest 2 days after treatment with 1 mmol/l siRNA at the various dosages and times studied (Fig. 4*A* and *B*). Interestingly, suppression of CaMKII by siRNA injection significantly reduced the level of active caspase-3 in retinas of mice 2 months after induction of diabetes; 2 days after treatment, the levels were 1.9-, 2.1-, 1.6-, and 2.5-fold lower, respectively, in siRNA-injected diabetic mice com-

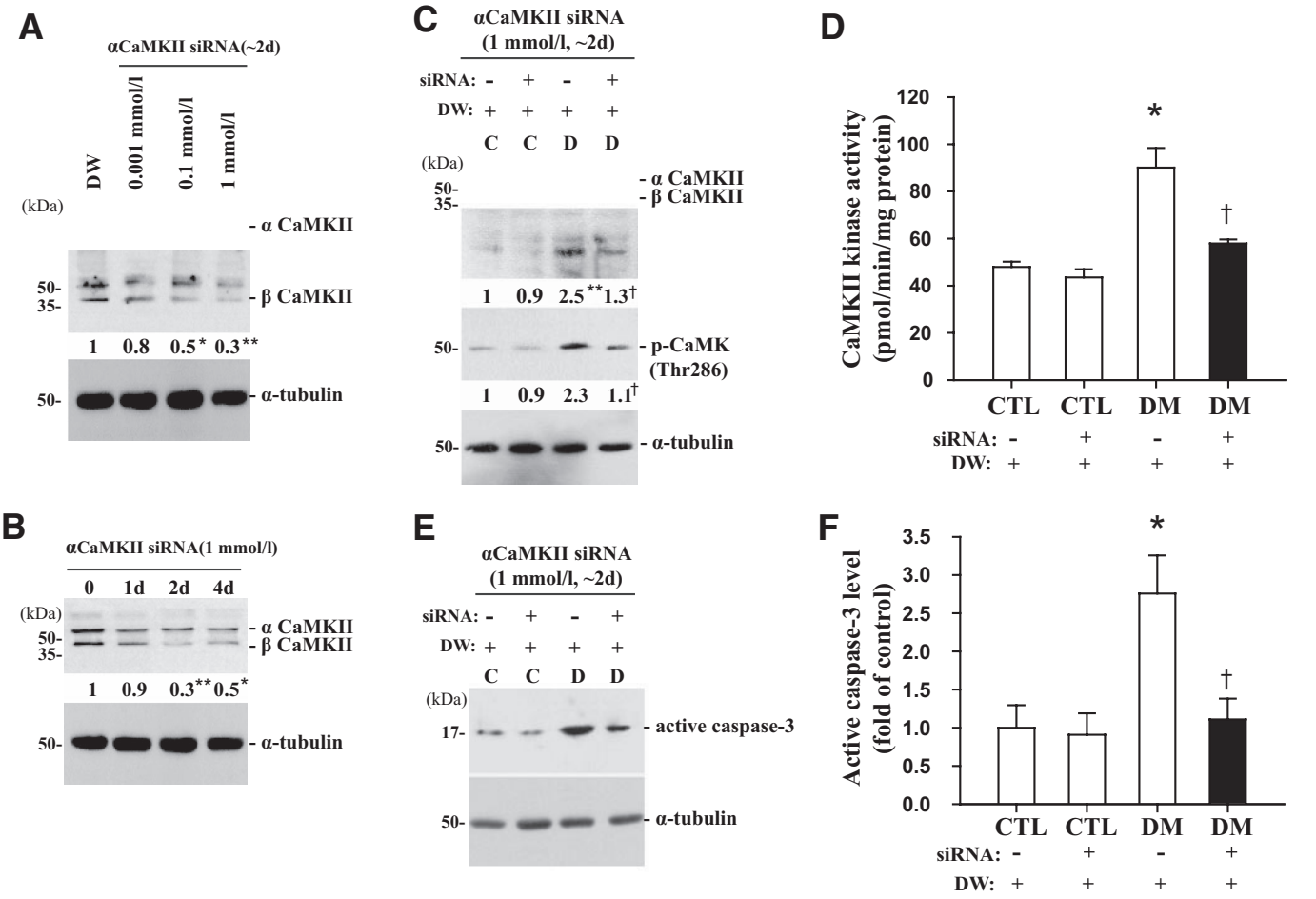

FIG. 4. Changes in CaMKII and phospho-CaMKII protein levels, kinase activity of CaMKII, and the level of active caspase-3 protein after αCaMKII knockdown using RNA interference in retinas of mice 2 months after induction of diabetes compared with controls. siRNA (2 μl) was injected into the right vitreous of the retinas, and an equal volume of distilled water was injected into the left vitreous as a control. *A* and *B*: Dose- and time-independent effects of siRNA on the level of CaMKII protein in the retinas of mice 2 months after the induction of diabetes, 2 days after injection with 0.01, 0.1, or 1 mmol/l siRNA, and 0, 1, 2, and 4 days after injection with 1 mmol/l siRNA using immunoblotting. *C–F*: Changes in CaMKII and phospho-CaMKII protein levels, CaMKII kinase activity, and active caspase-3 protein level in the retinas of control and diabetic groups, 2 days after the injection of 1 mmol/l αCaMKII siRNA. Each immunoblot was reprobed with α-tubulin, and levels of the other proteins were normalized to that of α-tubulin. The fold changes in protein levels compared with the controls (CTL) are indicated below the blots (*A–C*) or as a bar graph (*F*). DM, diabetic subjects. Results of the CaMKII kinase assay indicate the picomoles of phosphate incorporated into the CaMKII substrate peptide per minute per milligram of total protein (*D*). All data show representative results from four independent tests and are expressed as means ± SE ($n = 4$). *$P < 0.05$ and **$P < 0.001$ in *A*, comparing the DW-treated group with the others; *$P < 0.05$ and **$P < 0.001$ in *B*, comparing day 0 with the others; *$P < 0.05$ and **$P < 0.001$ in *C–F*, comparing the DW-treated control group with the others; †$P < 0.05$ in *C–F*, comparing the DW- and siRNA-treated diabetic groups. C and D, control and diabetic groups at 2 months after injection with STZ or buffer; DW, distilled water.

pared with mice injected with distilled water ($P < 0.05$, $n = 4$) (Fig. 4*C–F*). However, siRNA had no effect on control mice.

A specific CaMKII inhibitor, AIP (500 μmol/l), did not affect the level of CaMKII protein but greatly diminished the level of phospho-CaMKII in a time-dependent manner in the retinas of mice 2 months after induction of diabetes (Fig. 5*A*). The maximum decrease in the level of phospho-CaMKII protein was observed 2 days after the treatment at the various times studied. Finally, treatment with 500 μmol/l AIP greatly decreased the level of phospho-CaMKII protein, CaMKII kinase activity, and the level of active caspase-3 in the retinas of mice 2 months after induction of diabetes. Levels in AIP-treated diabetic mice were similar to those observed in control mice 2 days after injection (2.5-, 2-, and 5.5-fold lower, respectively, than in the PBS-treated diabetic group, $P < 0.05$, $n = 4$) (Fig. 5*B–E*). However, AIP had no effect on control mice.

Resveratrol treatment for 4 weeks blocked the increases in CaMKII and phospho-CaMKII protein levels and CaMKII kinase activity in the retinas of mice 2 months after induction of diabetes. Levels of CaMKII, phospho-CaMKII, and CaMKII activity were 1.7-, 1.8-, and 2-fold lower, respectively, in resveratrol-treated diabetic mice compared with CMC-treated diabetic mice ($P < 0.05$, $n = 4$) (Fig. 6*A–D*). Resveratrol also prevented the increase in the number of CaMKII and phospho-CaMKII immunopositive RGCs (arrows and arrowheads) in the retinas of mice 2 months after induction of diabetes, maintaining levels similar to those of controls. Levels of CaMKII and phospho-CaMKII were 2.2- and 3-fold lower, respectively, in resveratrol-treated diabetic mice compared with CMC-treated diabetic mice ($P < 0.05$, $n = 4$) (Fig. 6*H* and *L*).

Lastly, we found that resveratrol effectively prevented the increase in the level of active caspase-3 protein and the number of cells co-stained for TUNEL and phospho-CaMKII (arrows in Fig. 7*D* and *E*) in the retinas of mice 2

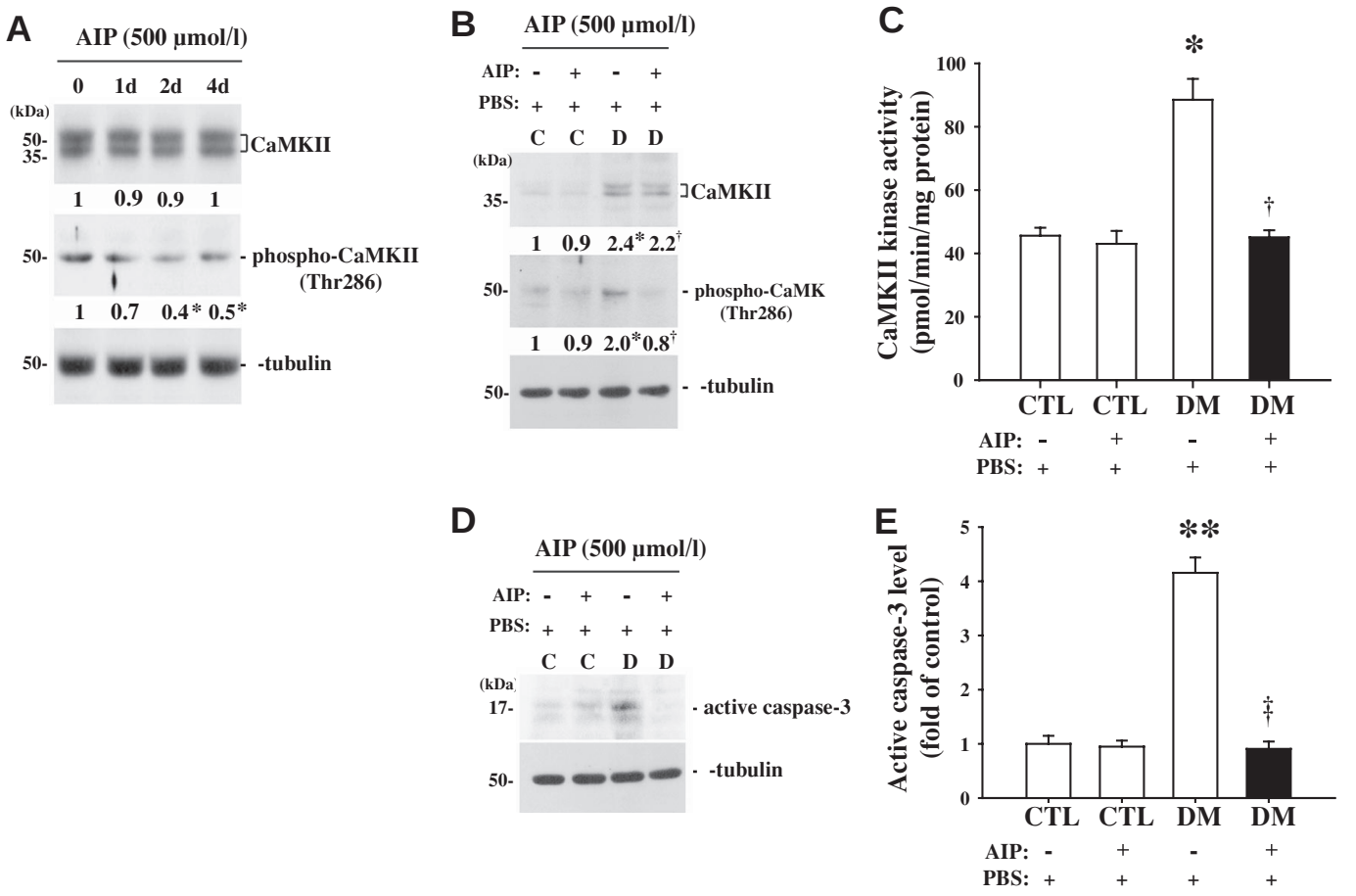

FIG. 5. Changes in CaMKII and phospho-CaMKII protein levels, kinase activity of CaMKII, and active caspase-3 protein level after AIP treatment of retinas of mice 2 months after induction of diabetes compared with controls. AIP (2 μl) was injected into the right vitreous in the retinas, and an equal volume of saline was injected into the left vitreous humor as a control. *A*: Western blot analysis of the time-independent effect of 500 μmol/l AIP on the CaMKII protein level in the retinas of mice 2 months after induction of diabetes at 0, 1, 2, and 4 days after AIP treatment. *B–E*: Changes in CaMKII and phospho-CaMKII protein levels, CaMKII kinase activity, and active caspase-3 protein level in the retinas of control and diabetic groups 2 days after AIP treatment. Each immunoblot was reprobed with α-tubulin, and the levels of other proteins were normalized to that of α-tubulin. The fold changes in protein levels compared with the controls (CTL) are indicated below the blots (*A* and *B*) or as a bar graph (*E*). DM, diabetic subjects. Results of the CaMKII kinase assay are indicated as picomoles of phosphate incorporated into the CaMKII substrate peptide per milligram of total protein (*C*). All data show representative results from four independent tests and are expressed as means ± SE ($n = 4$). *$P < 0.05$ in *A*, comparing day 0 with the others; *$P < 0.05$ and **$P < 0.001$ in *B–E*, comparing the saline-treated control group with the others; †$P < 0.05$ and ‡$P < 0.001$ in *B–E*, comparing the saline- and AIP-treated diabetic groups. C and D, control and diabetic groups 2 months after injection of STZ or buffer.

months after induction of diabetes. Levels of active caspase-3 and dying phospho-CaMKII–immunoreactive RGCs (arrowhead in insert) were 2.4- and 2.6-fold lower, respectively, in resveratrol-treated diabetic mice compared with CMC-treated diabetic mice ($P < 0.05$, $n = 4$) (Fig. 7*F*). However, resveratrol and CMC treatment did not significantly affect control or diabetic mice, respectively.

DISCUSSION

In the present study, we found that resveratrol effectively prevented diabetes-induced RGC death and CaMKII upregulation in type 1 diabetic mice.

Some investigators have suggested that neuronal damage in the retina could result from a reduction in retinal thickness, and a progressive loss of retinal structure in diabetes might contribute to the progression of diabetic neuropathy, resulting in vision loss (26,27). In this study, we confirmed that diabetes induces not only a reduction in inner retina thickness, including the GCL, but also the death of RGC cells (Fig. 1). It appears that the death of RGCs might be therefore linked to a decrease in the thickness of the inner retina, indicating that diabetes-induced retinal pathology occurred in our experimental model of diabetes.

CaMKII activation is involved in physiological and pathological events in neurons in an autophosphorylation-dependent manner (28,29). In particular, CaMKII action in damaged retinas is involved in the cell death pathway of RGCs, resulting in visual dysfunction (12,13,16). In the present study, we found that both total and phospho-CaMKII protein levels were increased, along with CaMKII activity, in retinas damaged by diabetes (Fig. 2). These results indicate that activation of CaMKII kinase depends on the elevated abundance of this enzyme in the diabetic retina. CaMKII and phospho-CaMKII immunoreactivity was detected only in RGCs throughout the retinas, and dying $TUNEL^+$ cells in the diabetic retinas were specific to immunopositive RGCs (Fig. 3). Our results are in agreement with those of many investigators who reported a proapoptotic function of CaMKII in retinal neurons (12,13,16). Phosphorylation of CaMKII has been known to play a pivotal role in the function of this enzyme, and CaMKII-selective siRNA (16,30) and potent inhibitors of CaMKII, such as AIP (10,12), have been used as tools to

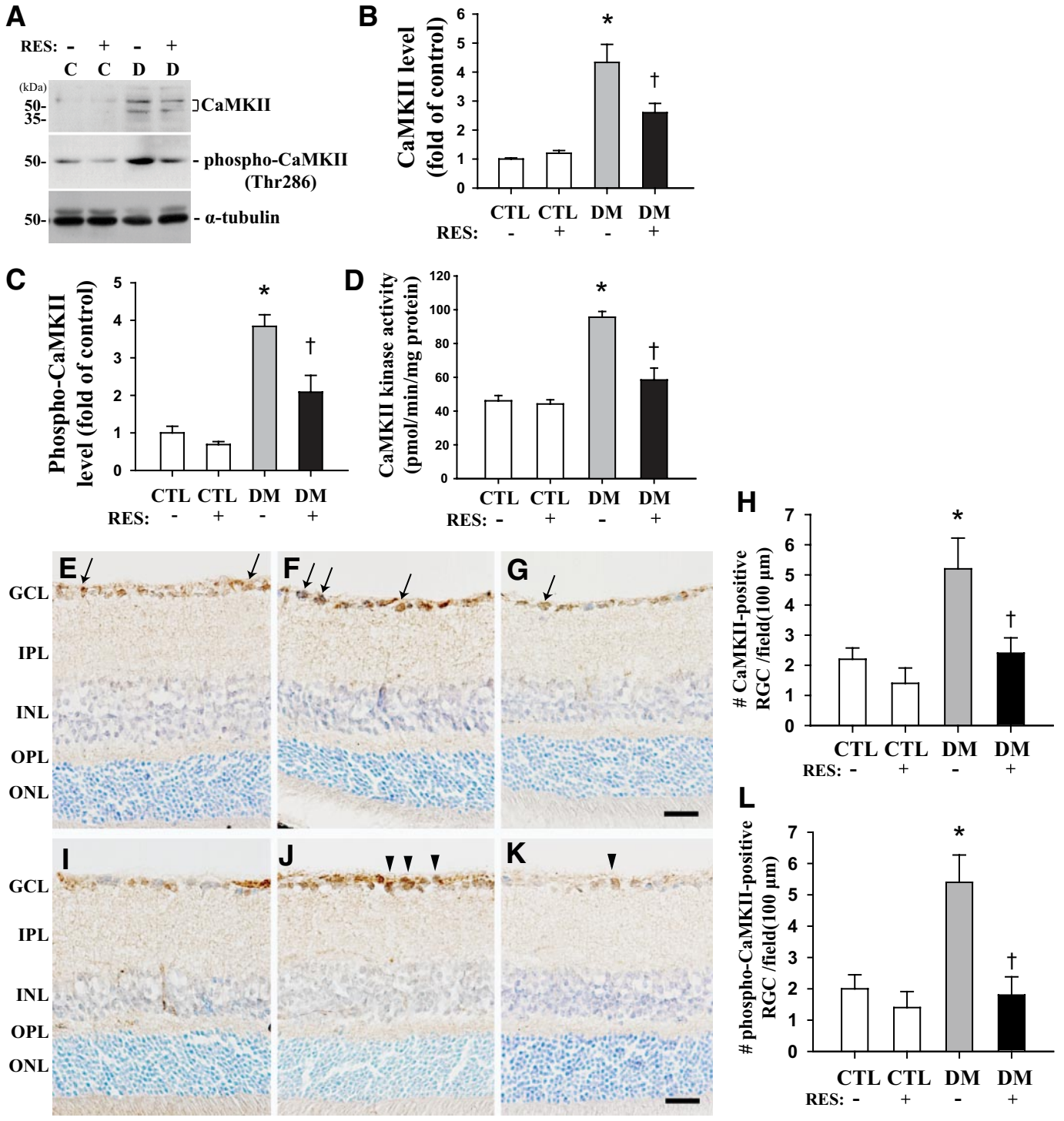

FIG. 6. Effects of resveratrol on CaMKII and phospho-CaMKII protein expression and the kinase activity of CaMKII in retinas of mice 2 months after induction of diabetes compared with controls. Resveratrol (20 mg · kg^{-1} · day^{-1}) was completely suspended in 0.5% CMC/0.9% saline and was administered by oral gavage once a day for 4 weeks, beginning 1 month from the last day of the fifth injection of STZ or buffer, and 0.5% CMC was used as a control. *A* shows representative immunoblots of CaMKII and phospho-CaMKII. Each immunoblot was reprobed with α-tubulin. The levels of the other proteins were normalized to that of α-tubulin, and the fold changes are indicated in *B* and *C*, respectively. Results of the CaMKII kinase assay are indicated in picomoles of phosphate incorporated into the CaMKII substrate peptide per minute per milligram of total protein (*D*). To confirm changes caused by resveratrol in CaMKII and phospho-CaMKII in neuronal cells of control and diabetic retinas, cryosections were immunostained with specific antibodies and counterstained with cresyl violet. Arrows and arrowheads indicate RGCs immunopositive for CaMKII (*E–G*) and phospho-CaMKII (*I–K*), respectively. The image of the resveratrol-treated control group was omitted from the figure because resveratrol and CMC treatment did not significantly affect control mice. The total number of these cells was counted in the GCL (~100 μm) in four different fields from three different retinas for each group (*H* and *L*). All data show representative results from four independent tests and are means ± SE ($n = 4$). *$P < 0.05$ and **$P < 0.001$, comparing the CMC-treated control group with the others; †$P < 0.05$ comparing the CMC- and resveratrol-treated diabetic groups. C (CTL) and D (DM), control and diabetic mice 2 months after injection of buffer or STZ; INL, inner nuclear layer; IPL, inner plexiform layer; ONL, outer nuclear layer; OPL, outer plexiform layer; RES, resveratrol. Bars, 12.5 μm. (A high-quality digital representation of this figure is available in the online issue.)

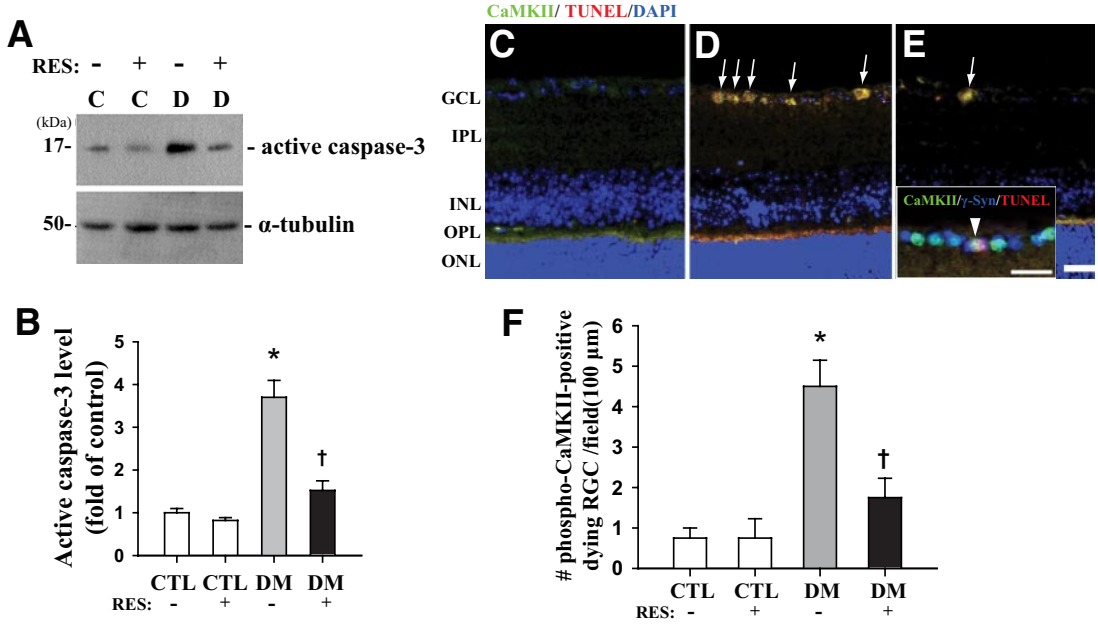

FIG. 7. Effects of resveratrol on cell death and RGC cells co-stained for TUNEL and phospho-CaMKII in retinas of mice 2 months after induction of diabetes compared with controls. *A* shows a representative immunoblot using antibody to active caspase-3. Each immunoblot was reprobed with α-tubulin. The levels of other proteins were normalized to that of α-tubulin, and the fold changes are indicated in *B*. To confirm the death of cells in conjunction with phospho-CaMKII expression, immunofluorescent staining of phospho-CaMKII using Alexa Fluor 488 goat anti-rabbit IgG (*green*) and TUNEL staining (*red*) were performed consecutively in the same sections, and the sections were counterstained with the nuclear marker DAPI (*C–E*). Arrows indicate TUNEL$^+$ cells that are immunopositive for phospho-CaMKII in the retinas of diabetic mice without or with resveratrol. To examine whether the co-positive cells were RGC cells, we performed sequential double-immunofluorescent staining for γ-Syn, the ganglion cell marker, and phospho-CaMKII, using Alexa Fluor 350 (*blue*) and 488 (*green*) goat anti-rabbit and -mouse IgGs before TUNEL staining (*red*). The arrowheads in the insert show the triple-stained RGC cell in the diabetic retina (*D*). Image of the resveratrol-treated control group was omitted from the figure because resveratrol and CMC treatment did not significantly affect control mice. The total number of double-stained cells was counted in the GCL (~100 μm) in four different fields from three different retinas for each group (*F*). Data are means ± SE ($n = 4$). *$P < 0.05$ comparing the CMC-treated control group with the others. †$P < 0.05$ comparing the CMC- and resveratrol-treated diabetic groups. C (CTL) and D (DM), control and diabetic mice 2 months after injection with buffer or STZ; INL, inner nuclear layer; IPL, inner plexiform layer; ONL, outer nuclear layer; OPL, outer plexiform layer; RES, resveratrol. Bars, 12.5 μm. (A high-quality digital representation of this figure is available in the online issue.)

study the physiological effects of CaMKII. In addition, AIP is known to confer neuroprotection on RGCs by inhibiting CaMKII autophosphorylation (12–14). In the present study, CaMKII siRNA and AIP treatments effectively prevented CaMKII activation, and these treatments also effectively attenuated RGC death induced by diabetes (Figs. 4 and 5). Together, our results indicate that diabetes-induced RGC death is primarily mediated by CaMKII overexpression and/or activation. However, CaMKII activation by phosphorylation also contributes to neuronal survival under certain conditions (15,16). For instance, activation of CaMKII may be a neuroprotective response against glutamate or its analog N-methyl-D-aspartate (NMDA)-induced retinal neurotoxicity both in vitro and in vivo (13,16). This discrepancy may be due to differences in neuronal sensitivity against different pathophysiological stimuli.

Recently, Deng et al. (31) suggested that resveratrol can partly block hyperglycemia via the enhancement of glucose uptake, and resveratrol is recognized as a potent clinical therapeutic for the treatment of diabetes-induced vascular dysfunction and cell death (32–34). Consistent with these results, we found that resveratrol significantly diminished the elevation in blood glucose levels in mice 2 months after induction of diabetes, although resveratrol-treated diabetic mice sustained a hyperglycemic state (Table 1). Therefore, we cannot exclude the possibility that resveratrol partially protects diabetes-induced retinal damage through the reduction of blood glucose levels but elicits effects that are not always coincident with the control of hyperglycemia.

The antidiabetic metabolic effects of resveratrol have been well documented in other organs besides the retina. Sirtuin 1 (SIRT1) and activator of AMP-activated protein kinase (AMPK), which are activated by resveratrol, have been described as key contributors to the protective effects of resveratrol in diabetic pathophysiology (19–21,35). Furthermore, a recent study reported that resveratrol promotes AMPK activation by CaMK kinase (CaMKK) (36). In a preliminary study, we examined effects of resveratrol on SIRT1 and AMPK levels in retinas of mice 2 months after induction of diabetes. Finally, we found that neither diabetes nor resveratrol affect SIRT1 action in our animal model and that phospho-AMPK levels were greatly lower in the retinas of diabetic mice than controls, and this decline was reversed by resveratrol treatment; however, phospho-AMPK levels in the retinas of resveratrol-treated diabetic mice were still in a state of significant decline compared with controls (all data not shown). These results suggest that resveratrol partly contributes to AMP kinase induction in our model; however, in the present study, activation of CaMKII induced by diabetes in mouse retinas was prevented and preserved at a basal level by resveratrol treatment (Figs. 6 and 7). Therefore, we suggest that AMPK is not likely to be a major target of resveratrol in CaMKII-mediated cell death in our animal experimental model. The discrepancy between our results

and those of other researchers may be due to differences in the pathophysiological conditions mediated by diabetes.

Recent studies have shown that resveratrol prevents RGC damage in response to various stresses, including oxidation and inflammation (22,23). Levels of cyclooxygenase-2 (COX-2) and inducible nitric oxide synthase (iNOS), regarded as indicators of these stresses, are increased in diabetic retinas in our model; these immunoreactivities were specific to vessels in retinas but not to neurons, and resveratrol decreases the induction of COX-2 and iNOS in diabetic retinas (data not shown). These data show that iNOS and COX-2 do not contribute to prevent retinal neurons from diabetes-induced cell death in our animal model, although we cannot rule out the possibility that resveratrol may affect biological processes through a reduction of oxidative stress and inflammation. Further, the present study showed that the oral administration of resveratrol effectively blocks the activation of CaMKII and RGC death in retinas damaged by diabetes (Figs. 5–7). Xu et al. (37) demonstrated that curcumin, another polyphenol with resveratrol-like physiological properties, regulates both CaMKII action and CaMKII-mediated RGC loss. Many studies have assessed the neuroprotective effects of natural polyphenolic components, including resveratrol, on chronic diseases such as diabetes (22,23,37–39). In addition, recent reports have indicated that a voltage-gated calcium channel can modulate calcium-dependent gene expression, including CaMKII, via activity-dependent transcriptional regulation (40) and that activation of CaMKII by voltage-gated calcium channels might contribute to the death of neuronal cells, including RGCs (41,42). However, considerable evidence has suggested that the protective effects of resveratrol from several stresses may be related to the direct inhibition of Ca^{2+} influx through the blockade of a voltage-gated calcium channel (43,44). Accordingly, we suggest that resveratrol might control CaMKII expression and activity through interference of a calcium- and voltage-gated calcium channel–dependent process.

Taken together, our data show that CaMKII is a potential target for the treatment of vision loss due to diabetes-induced neuropathy, and resveratrol is one such molecule that elicits protective effects against diabetes-induced retinal neuronal death via CaMKII suppression.

ACKNOWLEDGMENTS

This study was supported by the BK21 Program, a grant from the Korea Healthcare Technology R&D Project, Ministry for Health, Welfare & Family Affairs, Republic of Korea (A084575), and partially supported by the Medical Research Center for Neural Dysfunction program of the Ministry of Science & Technology/Korea Science and Engineering Foundation (MOST/KOSEF) (R13-2005-012-01001-1).

No potential conflicts of interest relevant to this article were reported.

We are grateful to Dr. Woong Sung for a critical reading of the manuscript and to Prof. Jang-Rak Kim for consulting on statistical analyses.

REFERENCES

1. Krady JK, Basu A, Allen CM, Xu Y, LaNoue KF, Gardner TW, Levison SW. Minocycline reduces proinflammatory cytokine expression, microglial activation, and caspase-3 activation in a rodent model of diabetic retinopathy. Diabetes 2005;54:1559–1565
2. Oshitari T, Hata N, Yamamoto S. Endoplasmic reticulum stress and diabetic retinopathy. Vasc Health Risk Manag 2008;4:115–122
3. Kern TS, Barber AJ. Retinal ganglion cells in diabetes. J Physiol 2008;586:4401–4408
4. Feit-Leichman RA, Kinouchi R, Takeda M, Fan Z, Mohr S, Kern TS, Chen DF. Vascular damage in a mouse model of diabetic retinopathy: relation to neuronal and glial changes. Invest Ophthalmol Vis Sci 2005;46:4281–4287
5. Zheng L, Gong B, Hatala DA, Kern TS. Retinal ischemia and reperfusion causes capillary degeneration: similarities to diabetes. Invest Ophthalmol Vis Sci 2007;48:361–367
6. Ali TK, Matragoon S, Pillai BA, Liou GI, El-Remessy AB. Peroxynitrite mediates retinal neurodegeneration by inhibiting nerve growth factor survival signaling in experimental and human diabetes. Diabetes 2008;57:889–898
7. Kim YH, Kim YS, Park CH, Chung IY, Yoo JM, Kim JG, Lee BJ, Kang SS, Cho GJ, Choi WS. Protein kinase C-delta mediates neuronal apoptosis in the retinas of diabetic rats via the Akt signaling pathway. Diabetes 2008;57:2181–2190
8. Barber AJ, Lieth E, Khin SA, Antonetti DA, Buchanan AG, Gardner TW. Neural apoptosis in the retina during experimental and human diabetes: early onset and effect of insulin. J Clin Invest 1998;102:783–791
9. Gao J, Duan B, Wang DG, Deng XH, Zhang GY, Xu L, Xu TL. Coupling between NMDA receptor and acid-sensing ion channel contributes to ischemic neuronal death. Neuron 2005;48:635–646
10. Goebel DJ. Selective blockade of CaMKII-alpha inhibits NMDA-induced caspase-3-dependent cell death but does not arrest PARP-1 activation or loss of plasma membrane selectivity in rat retinal neurons. Brain Res 2009;1256:190–204
11. Gu Z, Liu W, Yan Z. Beta-amyloid impairs AMPA receptor trafficking and function by reducing Ca2+/calmodulin-dependent protein kinase II synaptic distribution. J Biol Chem 2009;284:10639–10649
12. Fan W, Agarwal N, Kumar MD, Cooper NG. Retinal ganglion cell death and neuroprotection: involvement of the CaMKIIalpha gene. Brain Res Mol Brain Res 2005;139:306–316
13. Fan W, Agarwal N, Cooper NG. The role of CaMKII in BDNF-mediated neuroprotection of retinal ganglion cells (RGC-5). Brain Res 2006;1067:48–57
14. Fan W, Cooper NG. Glutamate-induced NFkappaB activation in the retina. Invest Ophthalmol Vis Sci 2009;50:917–925
15. Fan W, Li X, Cooper NG. CaMKIIalphaB mediates a survival response in retinal ganglion cells subjected to a glutamate stimulus. Invest Ophthalmol Vis Sci 2007;48:3854–3863
16. Takeda H, Kitaoka Y, Hayashi Y, Kumai T, Munemasa Y, Fujino H, Kobayashi S, Ueno S. Calcium/calmodulin-dependent protein kinase II regulates the phosphorylation of CREB in NMDA-induced retinal neurotoxicity. Brain Res 2007;1184:306–315
17. King RE, Kent KD, Bomser JA. Resveratrol reduces oxidation and proliferation of human retinal pigment epithelial cells via extracellular signal-regulated kinase inhibition. Chem Biol Interact 2005;151:143–149
18. Ohgami K, Ilieva I, Shiratori K, Koyama Y, Jin XH, Yoshida K, Kase S, Kitaichi N, Suzuki Y, Tanaka T, Ohno S. Anti-inflammatory effects of aronia extract on rat endotoxin-induced uveitis. Invest Ophthalmol Vis Sci 2005;46:275–281
19. Zang M, Xu S, Maitland-Toolan KA, Zuccollo A, Hou X, Jiang B, Wierzbicki M, Verbeuren TJ, Cohen RA. Polyphenols stimulate AMP-activated protein kinase, lower lipids, and inhibit accelerated atherosclerosis in diabetic LDL receptor-deficient mice. Diabetes 2006;55:2180–2191
20. Lee JH, Song MY, Song EK, Kim EK, Moon WS, Han MK, Park JW, Kwon KB, Park BH. Overexpression of SIRT1 protects pancreatic beta-cells against cytokine toxicity by suppressing the nuclear factor-kappaB signaling pathway. Diabetes 2009;58:344–351
21. Sharma SS, Kumar A, Arora M, Kaundal RK. Neuroprotective potential of combination of resveratrol and 4-amino 1,8 naphthalimide in experimental diabetic neuropathy: focus on functional, sensorimotor and biochemical changes. Free Radic Res 2009;43:400–408
22. Shindler KS, Ventura E, Rex TS, Elliott P, Rostami A. SIRT1 activation confers neuroprotection in experimental optic neuritis. Invest Ophthalmol Vis Sci 2007;48:3602–3609
23. Liu Q, Ju WK, Crowston JG, Xie F, Perry G, Smith MA, Lindsey JD, Weinreb RN. Oxidative stress is an early event in hydrostatic pressure induced retinal ganglion cell damage. Invest Ophthalmol Vis Sci 2007;48:4580–4589
24. Kim YH, Kim YS, Kang SS, Noh HS, Kim HJ, Cho GJ, Choi WS. Expression of 14–3-3 zeta and interaction with protein kinase C in the rat retina in early diabetes. Diabetologia 2005;48:1411–1415
25. Kim YH, Kim YS, Noh HS, Kang SS, Cheon EW, Park SK, Lee BJ, Choi WS, Cho GJ. Changes in rhodopsin kinase and transducin in the rat retina in early-stage diabetes. Exp Eye Res 2005;80:753–760
26. Martin PM, Roon P, Van Ells TK, Ganapathy V, Smith SB. Death of retinal

neurons in streptozotocin-induced diabetic mice. Invest Ophthalmol Vis Sci 2004;45:3330–3336
27. van Dijk HW, Kok PH, Garvin M, Sonka M, Devries JH, Michels RP, van Velthoven ME, Schlingemann RO, Verbraak FD, Abràmoff MD. Selective loss of inner retinal layer thickness in type 1 diabetic patients with minimal diabetic retinopathy. Invest Ophthalmol Vis Sci 2009;50:3404–3409
28. Yamagata Y, Imoto K, Obata K. A mechanism for the inactivation of Ca2+/calmodulin-dependent protein kinase II during prolonged seizure activity and its consequence after the recovery from seizure activity in rats in vivo. Neuroscience 2006;140:981–992
29. Sasaki T, Han F, Shioda N, Moriguchi S, Kasahara J, Ishiguro K, Fukunaga K. Lithium-induced activation of Akt and CaM kinase II contributes to its neuroprotective action in a rat microsphere embolism model. Brain Res 2006;1108:98–106
30. Zayzafoon M, Fulzele K, McDonald JM. Calmodulin and calmodulin-dependent kinase IIalpha regulate osteoblast differentiation by controlling c-fos expression. J Biol Chem 2005;280:7049–7059
31. Deng JY, Hsieh PS, Huang JP, Lu LS, Hung LM. Activation of estrogen receptor is crucial for resveratrol-stimulating muscular glucose uptake via both insulin-dependent and -independent pathways. Diabetes 2008;57:1814–1823
32. Thirunavukkarasu M, Penumathsa SV, Koneru S, Juhasz B, Zhan L, Otani H, Bagchi D, Das DK, Maulik N. Resveratrol alleviates cardiac dysfunction in streptozotocin-induced diabetes: role of nitric oxide, thioredoxin, and heme oxygenase. Free Radic Biol Med 2007;43:720–729
33. Gan L, Matsuura H, Ichiki T, Yin X, Miyazaki R, Hashimoto T, Cui J, Takeda K, Sunagawa K. Improvement of neovascularization capacity of bone marrow mononuclear cells from diabetic mice by ex vivo pretreatment with resveratrol. Hypertens Res 2009;32:542–547
34. Palsamy P, Subramanian S. Modulatory effects of resveratrol on attenuating the key enzymes activities of carbohydrate metabolism in streptozotocin-nicotinamide-induced diabetic rats. Chem Biol Interact 2009;179:356–362
35. Hou X, Xu S, Maitland-Toolan KA, Sato K, Jiang B, Ido Y, Lan F, Walsh K, Wierzbicki M, Verbeuren TJ, Cohen RA, Zang M. SIRT1 regulates hepatocyte lipid metabolism through activating AMP-activated protein kinase. J Biol Chem 2008;283:20015–20026
36. Vingtdeux V, Giliberto L, Zhao H, Chandakkar P, Wu Q, Simon JE, Janle EM, Lobo J, Ferruzzi MG, Davies P, Marambaud P. AMP-activated protein kinase signaling activation by resveratrol modulates amyloid-beta peptide metabolism. J Biol Chem 2010;285:9100–9113
37. Xu Y, Lin D, Li S, Li G, Shyamala SG, Barish PA, Vernon MM, Pan J, Ogle WO. Curcumin reverses impaired cognition and neuronal plasticity induced by chronic stress. Neuropharmacology 2009;57:463–471
38. Lin HJ, Lai CC, Lee Chao PD, Fan SS, Tsai Y, Huang SY, Wan L, Tsai FJ. Aloe-emodin metabolites protected N-methyl-d-aspartate-treated retinal ganglion cells by Cu-Zn superoxide dismutase. J Ocul Pharmacol Ther 2007;23:152–171
39. Ates O, Cayli SR, Yucel N, Altinoz E, Kocak A, Durak MA, Turkoz Y, Yologlu S. Central nervous system protection by resveratrol in streptozotocin-induced diabetic rats. J Clin Neurosci 2007;14:256–260
40. Chang KT, Berg DK. Voltage-gated channels block nicotinic regulation of CREB phosphorylation and gene expression in neurons. Neuron 2001;32:855–865
41. Hao ZB, Pei DS, Guan QH, Zhang GY. Calcium/calmodulin-dependent protein kinase II (CaMKII), through NMDA receptors and L-Voltage-gated channels, modulates the serine phosphorylation of GluR6 during cerebral ischemia and early reperfusion period in rat hippocampus. Brain Res Mol Brain Res 2005;140:55–62
42. Ko ML, Liu Y, Dryer SE, Ko GY. The expression of L-type voltage-gated calcium channels in retinal photoreceptors is under circadian control. J Neurochem 2007;103:784–792
43. Chen YC, Nagpal ML, Stocco DM, Lin T. Effects of genistein, resveratrol, and quercetin on steroidogenesis and proliferation of MA-10 mouse Leydig tumor cells. J Endocrinol 2007;192:527–537
44. Szkudelski T. Resveratrol-induced inhibition of insulin secretion from rat pancreatic islets: evidence for pivotal role of metabolic disturbances. Am J Physiol Endocrinol Metab 2007;293:E901–E907